RAI 2-1

The staff asked the applicant to better explain the conservatisms assumed in the end drop analysis and to provide additional details about the assumptions used to model the block and the unyielding surface (e.g., material). The applicant indicated that it provided the material's properties in the report. The applicant also indicated that it performed a finite element analysis with the material properties. The staff asked the applicant to provide a summary of its finite element analysis using the LSDYNA code and explain modeling assumptions as well as results. As the RAI requested, the response should include both qualitative and quantitative descriptions of the end drop analysis, the damage experience of the package (including the fuel), and explanations of how the analysis meets the regulations in 10 CFR Part 71.

AREVA Response

Model Summary

As discussed the analysis performed by Atkins for AREVA in Reference 2-1-1 to demonstrate that the analysis meets the regulations in 10 CFR Part 71, the acceleration of the 30-ft drop specified in 10 CFR Part 71 is used as input to check the structural stability criteria based on the plastic load analysis methodology specified in ASME Code 2010, Subsection III, Appendix F. Section F-1341.4. The ASME Code states that the allowable load should not exceed 70% of the plastic instability load. Therefore if the structure can withstand an amplified compressive load that is 1.4 (=1/0.70) times of the actual peak load, then the minimum factor of safety is established to be 1.4. The criterion for the minimum safety factor for the Atrium-11 fuel bundle stability evaluation is considered to be 1.4 (1/0.7). It is also the ASME Code-required minimum factor of safety. To demonstrate that the analysis meets the regulations in 10 CFR Part 71, the acceptance criteria for the plastic stability of fuel bundle are established as follows.

1. During normal and accident temperature and pressure conditions, the fuel bundle cladding remains stable without gross deformation or collapse that can cause a criticality incident.
2. During the accident drop scenario, the geometry of the fuel bundle remains safe and will not cause criticality.

The analyses are performed using the LSDYNA finite element dynamic analysis program. As described in section 7 of Reference 2-1-1, for the evaluation of the TN-B1 shipping container, the LSDYNA finite element model used for the evaluation includes the outer container, inner container, fuel load, and the shock absorbing materials between the inner and outer containers and between the fuel and inner container. Generally, shell elements are used to represent the stainless steel structural of the inner and outer containers, and solid 3D brick elements are used to model the various wood components and other shock absorber blocks. Welds are not explicitly included in the model, but the connections between joined parts made of shell elements are represented using merged nodes. The geometry of the container model is determined from the AREVA drawings.

Additionally, two fuel assemblies are modeled as rigid rectangular blocks with a square cross-section and defined with the *MAT_RIGID material specification as the structural response of the fuel itself is not an objective of the container model. The TN-B1 overall finite element model and various components are shown in Figures 7.1-1 through 7.1-4 of Reference 2-1-1.

The interaction between all components is included with a single surface contact definition for all container parts, and a surface to surface contact definition for the container and rigid impact plane. For all drop analyses, impact of the container is on a rigid plane located just below the outer container. The rigid plane, defined with a *MAT_RIGID material specification, is modeled as a rectangular surface generated with shell elements and fixed in space. The rigid impact surface lies in the x-y plane, with the negative z-axis as the vertical drop direction. LSDYNA simulation commences at a time just before impact with the rigid plane. An initial downward velocity corresponding to the drop distance is applied to the entire model.

Modeling Assumptions

Assumptions used in the container model include the material properties validated using the instrumented 30-ft (9-meter) drop test performed on the RAJ-II Certification Test Unit (CTU) at room temperature. The RAJ-II CTU has the identical geometry and total gross weight (930 kg) as the AREVA TN-B1 shipping container. The weight of the fuel contents used in the CTU test is 560 Kg. The maximum weight of the ATRIUM-11 Fuel Assembly is 684 kg. The un-instrumented container drop test with fuel weight of 684 kg was performed at National Transportation Research Center (NTRC) in Oak Ridge, Tennessee. The results are used to compare with the damages of the analytical model. The validated finite element model with the design weight is used to simulate the structural performance of the container under NCT (1.2 meter drop) and HAC (9 meter drop) at -40^{O}F and 150^{O}F. The temperature conditions analyzed are more conservative than the 10CFR Code required value between -20^{O}F and 100^{O}F. The deceleration time history of the inner container is used for the subsequent fuel bundle drop analysis. The CTUs and test results are described in AREVA TN-B1 SAR FS-0014159 sections 2.5 and 2.12 respectively.

For the evaluation of the fuel bundle, the inner container is included only as rigid boundary. The fuel bundle is modeled in detail. The following contents inside the inner container are added to the fuel bundle finite element model. As shown in licensing drawing 105E3745 sheet 1 of 2, page 55 of Reference 2-1-2, the inner container has a protective layer between the fuel bundle and the inner container external shell. The protective layer consists of 1) End Face Lumber, Item #26 and 2) Thermal Insulator, Item #34. During the end drop simulation of the fuel bundles, the lumber and the thermal insulator are included in the finite element model. Therefore the fuel bundle is not impacting directly against the inner container shell, which is treated as a rigid body. During the side drop and corner drop simulation of the fuel bundles, the lumber and the thermal insulator are omitted and not modeled because of conservatism. The lumber and the thermal insulator are treated as elastic material in the TN-B1 shipping cask finite element analysis but they are treated as crushable foam material in the fuel bundle drop analysis.

Material Property of Lumber

The common lumber materials used in the inner container are soft woods, such as Hemlock or Redwood. The material properties of the lumber used in the packaging, with the exception of the dynamic effect on elastic modulus, are discussed in page A47, Section A.5 of Reference 2-1-1. A detail discussion of wood as impact absorbing material can be found in page 80, Section 4.3 of the report, "*Investigation of the Behavior of Shock-Absorbing Structural Parts of Transport Casks Holding Radioactive Substances in Terms of Design Testing and Risk Analysis*, Martin Neumann, BAM-Dissertation Series, Volume 45, Berlin, 2009". Under pressure parallel to the wood grain, the microscopic fibrous compression mechanism is discussed in detail in page 51, Section 3.2.3. In the public domain, there is a lack of research data on the material property of Hemlock wood under dynamic compressive load. However, in the same reference above, page 108, Figure 5.3, a typical applied stress-volumetric crush characteristic curve of wood sample is proposed as well as the stress function. The representative shape of the wood characteristic curve is reproduced below.

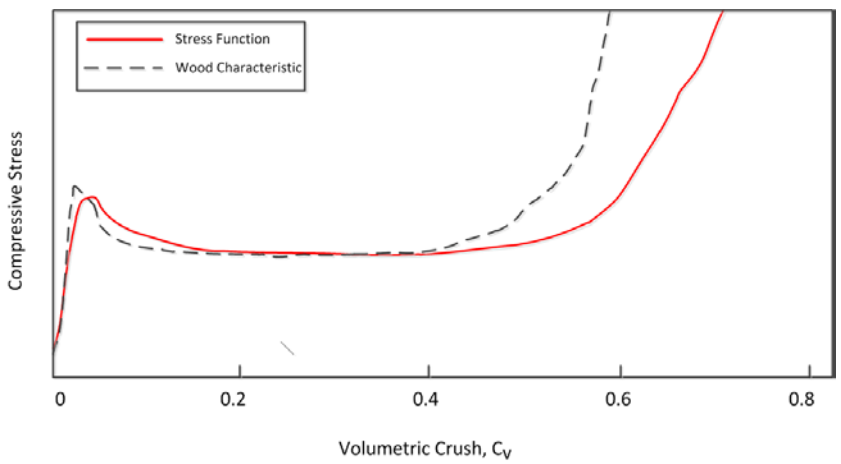

The volumetric crush is defined as $C_v=(1-V_1/V_o)$, where V_1 is the compressed volume and V_o is the original volume.

The applied stress-volumetric crush curve of the wood can be described using a simple model consisting of three distinct phases:

1. **Linear**, elastic response to initial crush. In this stage, the energy absorbing capability of the wood is very limited. At the end of this range, the compressive stress limit is reported as the breaking strength in the reference "*Wood Handbook, Wood as an Engineering Material, US Dept of Agriculture, FPL-GTR-190*".
2. **Plastic crush plateau**. As the pressure reaches the compressive strength limit of the wood, the wood volume would continue to compress with very small increase of the stress. In this phase, most of the impact energy is dissipated by the volumetric crush of the wood specimen.
3. **Densification**. The wood would eventually reach a state that an enormous increase of stress with very small reduction of wood volume. This condition is called a lock-up of the wood fiber and mostly occurs when the wood is compressed to about 40% of its original volume that $V_1=0.4V_o$. The volumetric crush is $C_v=(1-V_1/V_o) = (1-0.4V_o/V_o) =0.6$. This stage is represented by the steep slope in the above wood characteristic curve at or near volumetric crush $C_v=0.6$.

Developed from the above material model and the characteristics of observed actual wood sample test result of the above references, the applied compressive stress-volumetric crush for the axial compression of lumber is obtained and presented in the figure below. The sloped feature of the curve is implemented to improve the numerical stability of the LSDYNA program runs.

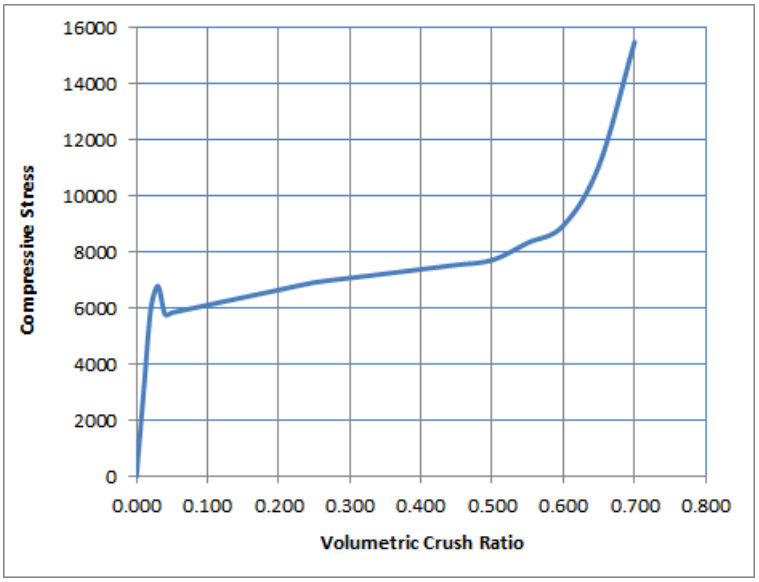

Figure: Compressive Stress-Volumetric Crush of Hemlock Wood

This material model has an average compressive stress of 7200 psi that matches the data in Appendix A.5 of Reference 2-1-1. For the cold temperature application, the stiffness of the wood is conservatively increased by 14%. This material is modeled as crushable foam in the LSDYNA program.

Material Property of Thermal Insulator

The material properties of the thermal insulator used in the inner container, with the exception of the dynamic effect on elastic modulus, are discussed in page A49, Section A.6 of Reference 2-1-1. The thermal insulator is a light weight fibrous material (specific gravity =0.25), therefore, under compressive load, the collapse mechanism of all fibrous material behaves as crushable foam or honeycomb. Based on the 10% volumetric crush strength of the thermal insulator presented in

Section 7.3.6.a of Reference 2-1-1, the compressive strength is 42.6 psi. Further assuming that the volumetric crush would respond in proportion to the applied compressive load (extrapolated results in the table below) until it reaches a lock-up state that an enormous increase of the applied stress would cause only a small increase of the volumetric crush. The volumetric crush at lock-up is conservatively assumed to be 60%. The table below shows the generated applied load vs. the volumetric crush. This material is modeled as crushable foam in the LSDYNA program.

Volumetric Crush	Applied Compressive load (psi)
0.000	0.0
0.050	21.3
0.100	42.6
0.150	63.9
0.300	127.8
0.500	1000.0
0.700	100000.0
0.900	500000.0

The finite element model of the fuel bundle is presented in page 10, Section 7.1 of Reference 2-1-3. For the current analysis, the rigid plane corresponds to the bottom shell of inner container. This modeling approach conservatively ignores the flexibility of the bottom shell of the inner container and the energy absorption capability of the balsa wood between the bottom shell of inner container and the outer container shell. The wood plate and thermal insulator inside the inner container are added to the finite element model between the lower tip of the fuel bundle lower tip plate and the bottom shell of inner container as shown in page B5, Section B.4 of Reference 2-1-1. The material properties of the fuel bundle are described in page 15, Section 7.3 of Reference 2-1-3. The material properties of the wood plate and insulator are described earlier in this response.

For the fuel bundle drop analyses, the drop configurations are described in page 21, Section 7.4 of the same reference. For the current analysis, no CG over corner drop is performed. Only the two most critical drops of end drop and side drops are performed.

The application of acceleration time histories for the drop input are described in page 25, Section 7.5 of the same reference. The actual acceleration time histories input for this confirmatory fuel bundle drop analysis are presented in page B2, Section B-2 of Reference 2-1-1. This confirmatory fuel bundle drop analyses are more conservative than the actual drop test because of amplified acceleration, material property, ambient temperature condition, and payload weight. For the boundary conditions, initial velocity and gravity load are described in page 30, Section 7.6 of Reference 2-1-3.

Results

From the drop test performed in Reference “GNF RAJ-II Licensing Application, SAR, Rev.7”, the comparison with drop analyses with previous fuel bundle drop analyses are shown in page 43, Section 7.8 of Reference 2-1-3. The qualitative damage to the package is described in page 54, Section 8 of Reference 2-1-1.

The predicted qualitative fuel bundle deformation from the current analysis is shown in page B6, Section B5 of Reference 2-1-1. From Figure B.5.1-1, it can be seen that the buckling of the fuel bundle tubes is very similar to that reported in page 44, Figure 7.8.2-1 of Reference2-1-3. The predicted fuel bundle deformation is more severe than the drop test result because the peak accelerations used for the drop analyses are magnified 1.4 times and the payload is heavier. However, the analysis result shows that while the outer container sustained damage and some deformation, the inner container remains intact without any inelastic strain.

The minimum ultimate strain of the material Zirconium used for the end plug and the cladding is 14% per reference No. 13 of Reference 2-1-1 , Page 23, Figure 16, [Review of Zircaloy-2 and Zircaloy-4 Properties Relevant to N.S. Savannah Reactor Design, Whitmorsh, July 9, 1962, ORNL-3281, UC-80-Reactor Technology, TID-4500, 17th Ed. C.L.]. The maximum plastic strain of the fuel rod is not reported in the drop test performed in Reference "GNF RAJ-II Licensing Application, SAR, Rev.7". The result of the current drop analysis shows the maximum plastic strain in the fuel cladding occurs at the weld and the heat-affected zone is 2.6% as shown in page B7, Figure B.5.1-2 of Reference 2-1-1. The maximum strain of 2.6% in the fuel rod is much less than the ultimate strain of 14% for the material Zirconium.

The strain conditions are summarized below.

Location	Cladding	Weld Heat Effected zone	End Plug Tip
Inelastic Strain	< 2.6%	2.6 %	12%
Ultimate Strain	14%	14%	14%
Factor of safety Based on 30-ft drop	>1.4x14/2.6=7.5	=1.4x14/2.6=7.5	Not applicable*

The multiplication factor of 1.4 in the above table is applied because the deceleration input has been amplified by a factor of 1.4. The inelastic strain at the tip of the end plugs is resulted from the end drop impact and has no effect on the structural integrity of the fuel cladding.

From the above summary, it is concluded that under the cold temperature condition, with the greater impact accelerations, the fuel assembly maintains its structural integrity of the cladding material without strain failure and also maintains a factor of safety of 1.4 against plastic instability. By complying with the ASME Code Structural Stability requirement under the Hypothetical Accident Condition specified in of 10 CFR Part 71, the shipping container design is in compliance with the Code requirement of 10 CFR Part 71.

References

2-1-1 FS1-0025122 "AREVA TN-B1 ATRIUM-11 Fuel Assembly Shipping Container Drop Analyses" Rev 1. This is ATKINS report ATKINS-NS-DAC-ARV-15-02 issued within AREVAs document control program. (Note 1)

2-1-2 FS1-0014159 "AREVA TN-B1 Docket No. 71-9372 Safety Analysis Report"

2-1-3 FS1-0015328 "Structural Analyses of the AREVA Atrium-11 LTA Fuel Assembly in the RAJ-II Container during Normal and Accident Transport Conditions" Rev 2. This is ATKINS report NSA-DAC-AREVA-14-01 Rev 1 issued within AREVAs document control program. (Note 1)

Note 1: These documents were previously submitted as a part of the original application for this revision. See AREVA letter TJT:16:-36 of 18 November 2016